Effect of pressure on the electron spin resonance of a heavy-fermion metal

J. Sichelschmidt, J. Wykhoff, T. Gruner, C. Krellner, C. Klingner, C. Geibel, and F. Steglich
Max Planck Institute for Chemical Physics of Solids, D-01187 Dresden, Germany

H.-A. Krug von Nidda, D. V. Zakharov, and A. Loidl
Experimental Physics V, Center for Electronic Correlations and Magnetism, University of Augsburg, D-86135 Augsburg, Germany

I. Fazlizhanov
E. K. Zavoisky Physical Technical Institute, 420029 Kazan, Russia

(Received 18 March 2010; revised manuscript received 3 May 2010; published 20 May 2010)

We investigate the electron-spin-resonance (ESR) phenomenon in the heavy-fermion metal $YbRh_2Si_2$ by applying hydrostatic pressure up to 3 GPa and by inducing the internal pressure on the Yb site chemically in $Yb(Rh_{1-x}Co_x)_2Si_2$ samples. We found that the increase in pressure, reducing the hybridization between $4f$ and conduction electrons, leads to a remarkable change in the temperature dependence of the g factor and broadens the ESR line. We relate the differences between the effect of internal and external pressure on the low-temperature ESR parameters to the disorder induced by Co doping. The pressure effects on the Yb^{3+}-related resonance in $YbRh_2Si_2$ again manifest its local character when compared with the resonance of diluted Gd in heavy-fermion metals.

DOI: 10.1103/PhysRevB.81.205116 PACS number(s): 76.30.−v, 71.27.+a

I. INTRODUCTION

The Kondo effect is now recognized to be of fundamental importance in a wide class of correlated electron systems. Experiments have demonstrated its significance not only in metals but also in nanoscale magnets, semiconductor quantum dots, carbon nanotubes, and individual molecules.[1] The discovery of a well-defined electron-spin-resonance (ESR) signal in a series of Kondo-lattice systems below the Kondo temperature T_K where heavy-fermion behavior begins to develop gives a unique opportunity to study the evolution of the Kondo state and heavy-fermion formation directly from the ESR measurables.[2–4] This is a strong advantage in contrast to earlier ESR experiments in Kondo lattices, which needed Gd doping as an ESR probe.[5] The origin and the unexpectedly small width of the absorption line are currently under intense theoretical investigations[6–11] which take into account that the ESR in Kondo-lattice systems is associated with the presence of ferromagnetic correlations.[3] These theories follow approaches within a Fermi-liquid[6] and non-Fermi-liquid[7,11] description of itinerant heavy electrons, utilize a Kondo-lattice model,[8] focus on the ESR signatures of the strongly anisotropic Kondo-ion interactions within a molecular-field description[9] or give a microscopic analysis of the spin dynamics of the Kondo ions.[10]

A particular interest was drawn to the ESR signal of the Kondo-lattice compound $YbRh_2Si_2$ (Ref. 2) which is located very close to a quantum critical point corresponding to the disappearance of weak antiferromagnetic (AFM) order.[12] The signal shows pronounced properties of a localized Yb^{3+} spin state but at the same time heavy-electron properties of the signal could be demonstrated by the signal dependence on the magnetic field.[4] Conduction electron (CE) spins and Yb^{3+} spins are strongly coupled and, hence, the ESR parameters were found to reflect changes in the hybridization between $4f$ and CE states when changing the unit-cell volume by substituting the Yb or Si sites with La or Ge, respectively.[13,14] However, these data could not provide conclusive results about the relation of the resonance linewidth to the hybridization strength, the Kondo interaction, and disorder scattering because in case of Ge doping only one concentration was available and La doping reduces the concentration of Yb^{3+} spins. Interestingly, the latter influenced the linewidth in a way very reminiscent to a so-called "bottleneck-relaxation" mechanism[14] which was indicated also by the ESR of Lu-doped $YbRh_2Si_2$ (Ref. 15) and which was discussed extensively for the spin dynamics of *diluted* magnetic moments in metallic hosts.[16] A recent microscopic description of the spin dynamics in $YbRh_2Si_2$ reflects a bottleneck relaxation in a dense Kondo system with strong anisotropic exchange interactions: a collective spin motion of the Kondo ions with conduction electrons was shown to explain the narrow linewidth by virtue of the Kondo effect.[10]

Here we report a systematic investigation of the ESR in $YbRh_2Si_2$ by a consecutive change in the hybridization strength by decreasing the unit-cell volume either by applying external hydrostatic pressure or by introducing chemical pressure by doping the Rh site with the isoelectronic but smaller Co ions. The latter allows to discriminate pure pressure effects from the effects of chemical modifications and disorder. As expected, pressure as well as Co doping stabilizes the antiferromagnetism in $YbRh_2Si_2$.[17]

Reports of ESR under pressure in metallic compounds are rare owing to the difficulty to achieve a high enough sensitivity. Up to now, there are only two studies available: the first one—of the metal-insulator transition in Yb:Eu by Continentino *et al.*,[18] the second one—of the spin-relaxation times in $CeAl_3$:Gd by Schlott *et al.*[19] It was shown that the external pressure strongly affects the hybridization strength, what leads to the opening of a conduction-band gap in ytterbium at 1.3 GPa and to an increase in the characteristic spin-fluctuation temperature T_0 in $CeAl_3$. In contrast to Ce systems, where the application of pressure strengthens the $4f$ conduction-electron hybridization and eventually generates

valence fluctuations, the $4f$ states in an Yb-based heavy-fermion system become more localized under pressure.[20] Such a picture successfully describes a *decrease* in T_0 from 25 to 8 K in $YbRh_2Si_2$ with pressures up to 1.7 GPa.[21,22]

II. EXPERIMENTAL SETUP

We measured the absorbed power P of a transversal magnetic microwave field (X band, $\nu \approx 9.4$ GHz) as a function of an external, static magnetic field H. To improve the signal-to-noise ratio, a lock-in technique was used by modulating the static field, which yielded the derivative of the resonance signal dP/dH. All ESR spectra were obtained from platelet-shaped single crystals with $H \perp c$ axis of the tetragonal crystal structure. The samples were prepared and thoroughly characterized as described elsewhere.[23–25]

High-pressure X-band ESR measurements were performed by means of a home-built hydraulic setup, which allows investigations in the pressure range up to 3 GPa.[26] The sample was placed in a Cu-Be gasket filled with a methanol-ethanol mixture. The gasket was compressed by two opposed Al_2O_3 anvils, one of which served simultaneously as a dielectric cylindrical cavity, operated at a TE_{111} mode. The use of a continuous-flow ^{4}He cryostat allowed to perform measurements in the temperature range 2.5–300 K. The pressure was determined from the jump in the ac resistivity at the superconducting transition of small pieces of lead which were put into the gasket together with the sample. The temperature was controlled with a calibrated carbon resistor. The X-band measurements of the Co-doped single crystals were performed at ambient pressure with a standard Bruker Elexsys Spectrometer equipped with a ^{4}He continuous gas-flow cryostat (Oxford instruments).

III. RESULTS

In accordance with previous experiments[2] all recorded ESR spectra consist of a single resonance line (see Fig. 1, symbols). We can satisfactorily describe the line by a Lorentzian line shape dP/dH (Refs. 27 and 28) (frequently called "Dysonian," solid lines in Fig. 1) which appears asymmetric due to the high sample conductivity giving rise to the skin effect which admixes dispersion to the absorption spectra. The skin depth was larger than 1 μm but, for all samples, much smaller than the sample thickness. We kept the ratio of dispersion to absorption constant, which is reasonable regarding the fact that the skin depth remains by far smaller than the sample dimensions in the temperature range under consideration. The line fits provided the parameters resonance field H_{res} and half linewidth at half maximum, ΔH. As displayed in Fig. 1 for $T=2.7$ K, both increasing pressure and Co concentration lead to a line broadening and a shift of H_{res} toward higher fields. External hydrostatic pressure qualitatively affects the ESR parameters in the same way as chemically induced pressure. For a pressure up to at least 0.6 GPa and a chemical pressure with a Co doping up to $x=0.03$ the corresponding ESR spectra are equivalent and can be described by the same g factors, see Fig. 2. In our pressure setup the ESR g factor, as calculated from the resonance

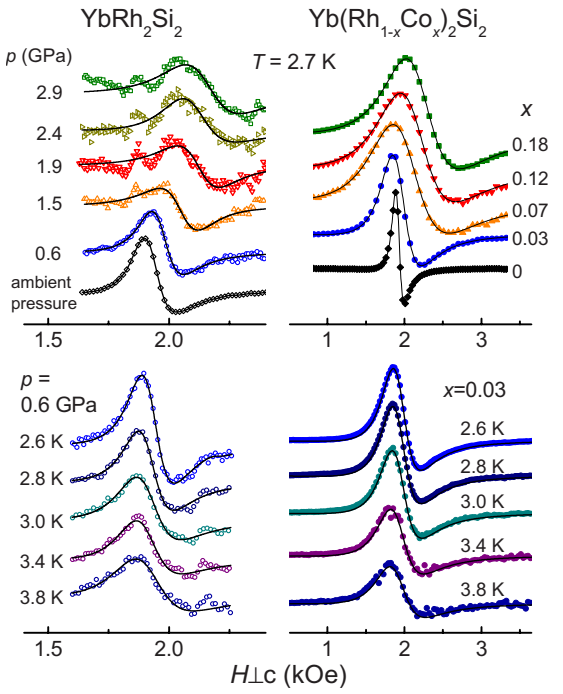

FIG. 1. (Color online) ESR spectra dP/dH (arbitrary units) of $Yb(Rh_{1-x}Co_x)_2Si_2$ at 9.4 GHz and $H \perp c$ with fitted Lorentzian shapes (solid lines). Amplitudes are scaled for best illustration. Top frames: $T=2.7$ K at various hydrostatic pressures p ($x=0$) and Co contents x ($p=0$). A weak signal near 1.8 kOe showing up for $p \geq 1.5$ GPa is due to the background of the pressure cell. Bottom frames: temperature dependence for $p=0.6$ GPa ($x=0$) and $x=0.03$ ($p=0$).

condition $h\nu = g\mu_B H_{res}$ (μ_B: Bohr magneton), amounts to $g_\perp = 3.485(6)$ at ambient pressure and $T=2.7$ K. This agrees well with the previously published value[2] in view of the different, higher quality batch of the crystal used here.

The dependence of the ESR parameters on hydrostatic pressure p and chemical pressure by Co doping x is displayed in Fig. 2 for $T=2.7$ K. The x and p values are related according the measured lattice parameters and the bulk

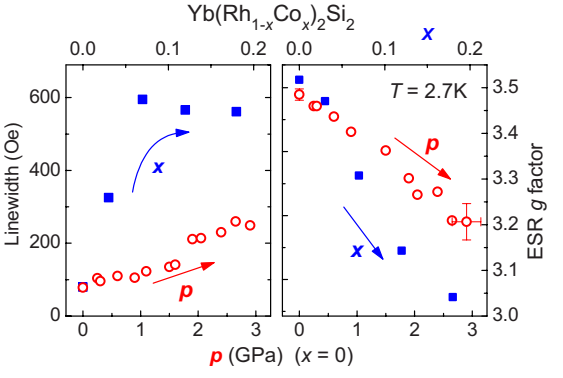

FIG. 2. (Color online) Linewidth and effective g factor of $Yb(Rh_{1-x}Co_x)_2Si_2$ at $T=2.7$ K and $H \perp c$. Open circles indicate the effect of hydrostatic pressure p for $x=0$ (lower axis), closed squares denote chemical pressure by a Co-doping concentration x at ambient hydrostatic pressure (upper axis). Error bars are given assuming the uncertainty in the resonance field as 10% of the linewidth.

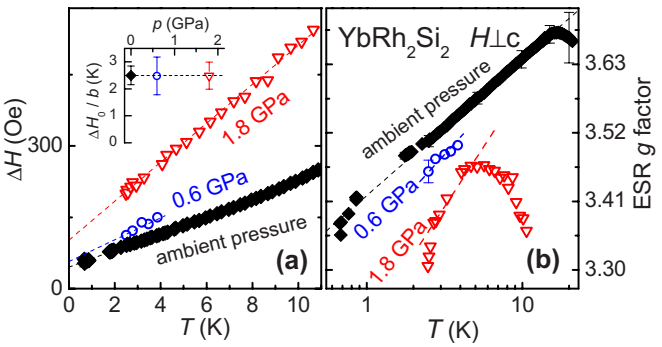

FIG. 3. (Color online) Temperature dependence at various hydrostatic pressures and field $H \perp c$ of (a) the linewidth ΔH and (b) the effective ESR g factor. Dashed lines in (a) display T-linear behavior of ΔH with slopes b and zero-temperature value ΔH_0 with $\Delta H_0/b \approx 2.5$ K as displayed in the inset. Dashed lines in (b) display log T dependencies of g (lines are guide to the eyes).

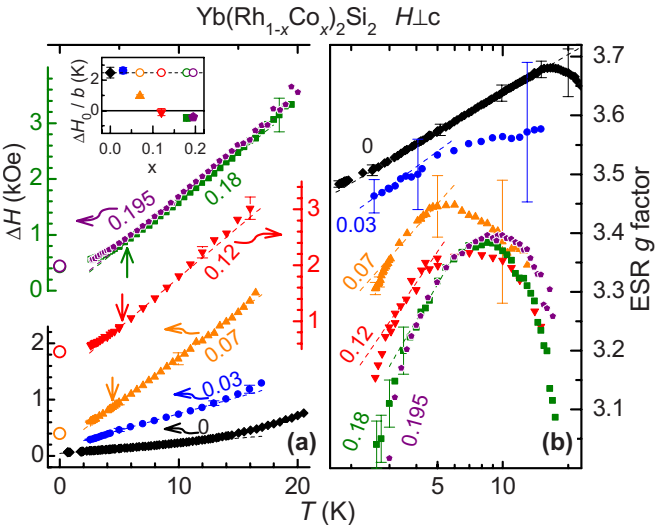

FIG. 4. (Color online) Temperature dependence at various chemical pressures induced by Co content x and field $H \perp c$ of (a) the linewidth ΔH and (b) the effective ESR g factor. Dashed lines display (a) T-linear behavior of ΔH with slopes b (deviation indicated by arrows) and (b) log T dependencies of g (guide to the eyes). Inset displays the ratio of zero-temperature linewidth ΔH_0 and b, where ΔH_0 arises from a linear linewidth extrapolation toward $T=0$ (solid symbols). The dashed line in the inset indicates $\Delta H_0/b \approx 2.5$ K (compare Fig. 3) which is used to determine the zero-temperature extrapolation of ΔH for $x \geq 0.07$ denoted by open circles.

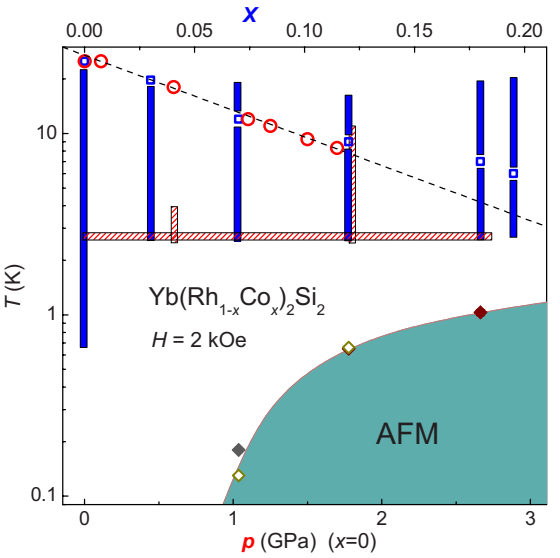

FIG. 5. (Color online) Temperature-pressure phase diagram at $H=2$ kOe (ESR X-band resonance field at $g=3.4$) showing the performed ESR measurements for various Co contents x (solid bars) and hydrostatic pressures p (shaded bars). The x and p values are linearly related according to the measured lattice parameters and the bulk modulus of $YbRh_2Si_2$ (Ref. 17). The dark shaded region indicates long-range AFM order (data from Refs. 21, 24, and 31). The Kondo temperature T_K is shown by the open circles (under pressure) and open squares (with Co doping) (data from Refs. 22, 24, and 25). The dashed line shows a Kondo-type temperature dependence $\exp(-0.7\ \mathrm{GPa}^{-1} \cdot p)$.

modulus of $YbRh_2Si_2$.[29] The relation could be confirmed by a perfect agreement of the transition temperatures of antiferromagnetic order of the Co-doped and pressurized samples.[17] As shown with the open symbols, increasing hydrostatic pressure leads to an increase in the linewidth from 80 Oe at ambient pressure to 250 Oe at $p=2.9$ GPa. At the same time the g factor shows an almost linear shift down to smaller values of 3.21(4) at $p=2.9$ GPa. The g factor in $Yb(Rh_{1-x}Co_x)_2Si_2$ coincides with the one in the parent compound at low Co concentrations $x<0.07$ but deviates to lower values for $x>0.07$. At $x=0.12$, it is shifted by ≈ -0.15 from the value at the corresponding pressure $p=1.8$ GPa, independently on temperature within experimental error [compare Figs. 3(b) and 4(b)]. This indicates that the ionic g value is reduced by Co doping and, concomitantly, the crystalline electric field should depend on Co doping as well. The typical linewidths in the Co-doped compounds are considerably larger than the linewidths at corresponding pressures and saturate to a value of about 600 Oe for $x \geq 0.07$. In this respect one should note the linear relationship between the residual linewidth and the electrical resistivity which was found for La-doped $YbRh_2Si_2$ (Ref. 14) and which we discuss for the Co-doped $YbRh_2Si_2$ in Sec. IV.

The temperature dependences of the ESR parameters were investigated at hydrostatic pressures of 0.6 and 1.8 GPa, and for Co concentrations up to $x=0.195$ (see illustration in Fig. 5). Figures 3(a) and 4(a) show the results for the ESR linewidth. The dashed lines indicate a linear law $\Delta H = \Delta H_0 + bT$ in a large T region, reminding to a Korringa law of local-moment relaxation toward conduction electrons[16] with parameters listed in Table I. Notable differences from the Korringa behavior occur above 12 K for $x=0$, indicating the influence of the first excited crystal-field level.[2] Interestingly, the linewidth data can be characterized by a ratio $\Delta H_0/b$ which indicates an interesting universal feature of the ESR relaxation as depicted in the insets of Figs. 3(a) and 4(a): $\Delta H_0/b \approx 2.5$ K remains almost unaffected by pressure and by Co doping up to $x=0.03$. Such behavior was previously already identified as a linewidth scaling of various $YbRh_2Si_2$ batches (which differ in their residual resistivities) and of La-doped $YbRh_2Si_2$ pointing to a common relaxation

TABLE I. Linewidth parameters of $\Delta H=\Delta H_0+bT$ obtained from linear fits as shown by the dashed lines in Figs. 3(a) and 4(a).

p (GPa)	x	ΔH_0 (kOe)	b (Oe/K)	$\Delta H_0/b$ (K)
Ambient	0	0.045	18	2.5 ± 0.35
0.6	0	0.057	23	2.5 ± 0.7
1.8	0	0.102	41	2.5 ± 0.5
Ambient	0.03	0.156	59	2.6 ± 0.2
Ambient	0.07	0.150	160	0.95 ± 0.1
Ambient	0.12	−0.02	180	-0.1 ± 0.2
Ambient	0.18	−0.09	170	-0.5 ± 0.2
Ambient	0.195	−0.075	175	-0.4 ± 0.2

mechanism to which both ΔH_0 and b can be ascribed.[14] For the ESR linewidth data of Co concentrations $x\geq0.07$ two characteristic differences to the corresponding pressure data are observable: First, a deviation from linearity occurs in the low-T region which is marked by arrows in Fig. 4. This deviation appears as soon as antiferromagnetic order at much lower temperatures has been established by Co doping, see phase diagram in Fig. 5. Second, the ratio $\Delta H_0/b$ strongly deviates from 2.5 K and even *negative* values of ΔH_0 appear for $x\geq0.12$ (see Table I). If one assumes the above-mentioned universal value $\Delta H_0/b\approx2.5$ K to hold also for $Yb(Rh_{1-x}Co_x)_2Si_2$ with $x\geq0.07$, one obtains values $\Delta H_0'$ which reasonably agree with the linewidth data at the lowest accessible temperatures [open circles in Fig. 4(a)].

The temperature dependence of the g factor under hydrostatic as well as chemical pressure is illustrated in Figs. 3(b) and 4(b). In the low-temperature region the dashed lines emphasize a logarithmic temperature dependence which could well describe the results for $YbRh_2Si_2$ at ambient pressure as was previously reported.[2] In the presence of antiferromagnetic order for pressures larger than 1 GPa (see Fig. 5) $g(T)$ deviates from a logarithmic decrease to a much stronger downturn, see the 1.8 GPa data in Fig. 3(b). In this respect two peculiarities are worth to note. For the data sets $x=0.12$ and the chemical pressure equivalent $p=1.8$ GPa the deviation appears at the same temperature of about 2.5 K, see Figs. 3(b) and 4(b). Furthermore, in case of the Co-doped samples these deviations appear at about the same temperatures where the linewidth departs from the linear temperature dependence, see arrows in Fig. 4(a).

IV. DISCUSSION

The phase diagram shown in Fig. 5 displays the parameter ranges of the ESR experiments under pressure (shaded bars) and Co doping (solid bars) together with magnetic and electronic properties. Applying pressure (either external hydrostatically or chemically by Co doping) suppresses the fluctuations of the Yb valence and leads to a decrease in the Kondo temperature T_K.[20] This effect is shown by the open circles and open squares which correspond to the characteristic spin-fluctuation temperature T_0 in the $4f$ increment of the low-temperature electronic specific heat $\Delta C/T\propto-\ln(T/T_0)$. At ambient pressure and zero field T_0 was shown to match with the single-ion Kondo temperature (obtained by evaluating the $4f$ entropy) (Ref. 30) and, hence, the temperature dependence of T_0 is consistent with an exponential law shown by the dashed line: $T_K\propto\exp[-1/JN_c(E_F)]$, where J is the exchange integral between $4f$ electrons and conduction electrons and $N_c(E_F)$ is the conduction-electron density of states at the Fermi surface, and assuming $x,p\propto1/JN_c(E_F)$.

Figure 1 demonstrates the qualitatively corresponding effect of pressure and Co doping on the ESR results which confirms that pressure effects are amenable with our ESR setup. The pressure effect on the temperature dependence of the linewidth can nicely be compared with the pressure effect on the ESR relaxation of diluted Gd^{3+} in Ce-Kondo-lattice systems, in $CeAl_3$, for instance.[19] There, both the magnetic susceptibility χ_{Ce} and the fluctuation time $\tau\propto1/T_K$ of the Ce $4f$ moments decrease by application of pressure. This effect could be detected in the low-temperature relaxation of the Gd^{3+} resonance: with increasing pressure the linewidth shows a decrease in the linear temperature slope $b\propto\chi_{Ce}/T_K$ and, simultaneously, a decrease in ΔH_0. A corresponding pressure effect, transferred to Yb systems,[20] is reflected by the linewidth behavior of $YbRh_2Si_2$. In agreement with the pressure-induced decrease in T_K (dashed line in Fig. 5) the slope b of the linewidth is increased by pressure and also, a simultaneous increase in ΔH_0 is observed [see Figs. 3(a) and 4(a)]. This equivalency points out that the ESR in $YbRh_2Si_2$ shows features of a local Yb^{3+} spin relaxation being influenced by the spin dynamics of the surrounding Yb^{3+} ions. A theoretical basis for understanding such signatures of locality in the linewidth-pressure dependences may be supplied by a recently developed model of the collective spin motion of $4f$- and conduction-electron spins in a Kondo lattice with strongly anisotropic Kondo interactions.[10] It reveals for the bottleneck regime a collective spin mode with a narrow linewidth showing the observed temperature dependence. In this model, besides the strong reduction in the linewidth by virtue of the Kondo effect, the line experiences also a "motional" narrowing process due to the translational diffusion of quasilocalized f electrons in the non-Fermi-liquid state. If the Ruderman-Kittel-Kasuya-Yosida interaction between nearest Yb ions is ferromagnetic, the diffusion process is supported and, hence, the linewidth depends also on the presence of short-range ferromagnetic fluctuations in $YbRh_2Si_2$. The application of pressure stabilizes antiferromagnetic correlations, leading to more localized f electrons and reduces the efficiency of the motional narrowing process. Within the phenomenology of a heavy-quasiparticle spin resonance the effect of ferromagnetic fluctuations on the quasiparticle scattering and spin-lattice relaxation was also found to significantly narrow the linewidth.[11] Furthermore, this framework stresses the role of the lattice coherence of the quasiparticles for effectively preventing a strong local relaxation of the Kondo spin. Therefore, regarding the different effect of Co doping and pressure for the absolute linewidth values one would expect a line broadening once the lattice coherence is disturbed by Co doping which, indeed, is observed, see Fig. 2. However, both approaches, describing the spin dynamics with a collective spin mode or within a quasiparticle picture,

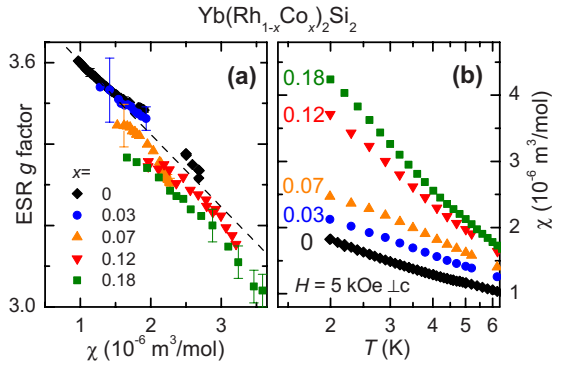

FIG. 6. (Color online) (a) ESR g values vs magnetic susceptibility χ indicates a linear relationship (dashed line: fit as described in the text) for different chemical pressures induced by Co content x. (b) $\chi(H=5$ kOe) vs temperature (log scale) at different chemical pressures.

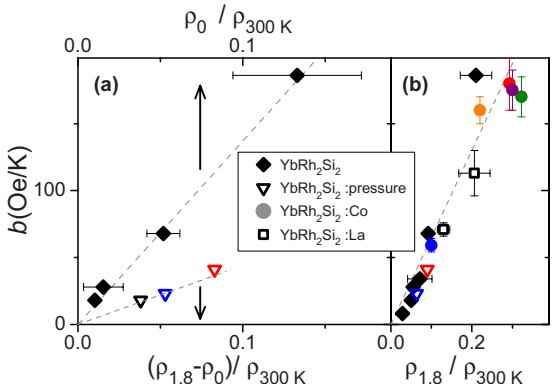

FIG. 7. (Color online) Variation in the linear temperature linewidth slope b with the ratios of electrical resistivity ρ at temperatures 1.8, 300, and 0.2 K (ρ_0). Closed diamonds correspond to $YbRh_2Si_2$ from different batches of indium flux grown crystals. Circles, triangles, and squares belong to samples with Co doping, under pressure, and with La doping (Ref. 14), respectively. Dashed lines are guide to the eyes.

have not yet explicitly considered the pressure variation in the Kondo temperature in their expressions for the linewidth and g factors.

Experimentally, a pressure-dependent Kondo scale is suggested by the observed dome shape of the g factor temperature dependence by application of pressure. With increasing temperature $g(T)$ reveals a logarithmiclike increase in a limited region of temperature which is followed by a substantial decrease. This happens at a temperature which is largest at ambient pressure and $x=0$ suggesting a relation of the dome position and the Kondo temperature. The theoretical considerations for a heavy-quasiparticle spin resonance indeed qualitatively predict such a dome in $g(T)$ in the non-Fermi-liquid regime which is determined by the temperature dependence of the quasiparticle effective mass and a contribution from a small anisotropy in the spin exchange.[11] From the low-temperature behavior of the g factor the collective spin-mode approach reveals a characteristic temperature for the ground Kramers doublet which is by two orders of magnitude smaller than the Kondo temperature.[10]

For all pressures the observed ESR g factors drop considerably below the insulator value g_0 expected for Yb^{3+} in $YbRh_2Si_2$. For the previous results at ambient pressure this negative shift was related to a negative, *antiferromagnetic* effective exchange coupling and a direct relation between the g factor and the static magnetic susceptibility was found.[2] Figure 6 shows that this is also the case for the Co-doped samples (appropriate susceptibility data under pressure were not available): the g values for various Co contents are shifted to smaller values proportional to the susceptibility. Such behavior cannot be explained by the effect of demagnetization which leads to a much weaker influence of the g factor ($\Delta g/g<0.5\%$ for $\Delta T=1$ K) and which, moreover, would correspond to an opposite temperature dependence of the g factor. Therefore, the temperature-dependent shift of the resonance could mostly be determined by the temperature dependence of internal antiferromagnetic exchange fields. A corresponding molecular-field approximation of the effective g factor, $g_{\mathrm{eff}}=g_0[1+\lambda\chi(T)]$, is indicated by the dashed line in Fig. 6(a) with $g_0=3.78$ (Ref. 32) and the molecular-field parameter $\lambda=-3.3$ kOe/μ_B which is consistent with the λ values estimated in Ref. 15. With increasing Co content from $x=0$ to $x=0.18$ one observes a parallel-like downshift of the $g(\chi)$ curves which corresponds to a decrease in g_0 of approximately 3% while a change in λ could not be resolved within the given experimental accuracy. The decrease in g_0 could be caused by changing the crystalline electric field with Co doping as was mentioned above, regarding the differences between the pressure- and doping-induced g shifts, see Fig. 2. The close relationship between the g factor and the magnetic susceptibility points out that the resonance reflects the local Yb^{3+} magnetic properties directly.

As was shown in Sec. III, the linewidth behavior under pressure is characterized by $\Delta H_0/b\approx 2.5$ K which provides evidence for a common relaxation mechanism involved in the residual linewidth ΔH_0 and the slope of the linear temperature dependence b. In this respect it is interesting to note the relation of both quantities to the residual electrical resistivity indicating the relevance of charge transport scattering processes for the ESR relaxation in $YbRh_2Si_2$. This was previously shown for ΔH_0 in Ref. 14 and is illustrated for b in Fig. 7. In order to discriminate the scattering effects from disorder and Kondo interaction, Fig. 7(a) compares b as a function of the disorder-dominated $\rho_0=\rho(0.2\ \mathrm{K})$ (upper axis) with the Kondo-dominated $\rho_{1.8\ \mathrm{K}}-\rho_0$ (lower axis). Whereas the effect of disorder variation should only show up among different $YbRh_2Si_2$ samples, the variation in the Kondo interaction should be dominant for the samples at various pressures. Indeed, as shown in Fig. 7(a), this situation is evidenced for the b values by their linear relation with the respective resistivity data. For the samples with La and Co doping, both disorder scattering and Kondo interaction contribute to b which then appears linearly related to $\rho_{1.8\ \mathrm{K}}/\rho_{300\ \mathrm{K}}$ as shown in Fig. 7(b). In particular, with $\Delta H_0'\approx b\cdot 2.5$ K, this behavior is also observable for the Co-doped samples with $x\geq 0.07$ and thus, the extrapolation of the residual linewidth values $\Delta H_0'$ shown by the open circles in Fig. 4(a) is also supported by $b\propto\rho_{1.8\ \mathrm{K}}/\rho_{300\ \mathrm{K}}$.

Nevertheless, the difference between the application of hydrostatic and chemical pressure for the electrical resistivity does not fully relate to the difference for the ESR parameters. This is most clearly indicated by the behavior of the linewidth toward low temperatures where the continuous linearity of the pressure data is in contrast to the presence of a kink in the Co data for $x \geq 0.07$ [arrows in Fig. 4(a)]. Interestingly, $x \geq 0.07$ also marks the lower bound for long-range AFM order (in the presence of an X-band resonance field of ≈ 2 kOe) as shown in the p-T phase diagram of Fig. 5 by the dark shaded area. Usually, when approaching magnetic ordering by lowering the temperature a slowing down of spin fluctuations results in a reduced narrowing process in the linewidth, i.e., in its increase. This provides a larger contribution from inhomogeneous broadening and is observed, for instance, for the resonance of Gd^{3+} in $Ce(Cu_{1-x}Ni_x)_2Ge_2$ ($x < 0.7$).[5] However, whether magnetic ordering is the dominant source for the arrow marked deviations of the $x \geq 0.07$ data, is questionable regarding the lack of deviation from linearity in the pressure linewidth data. Also, the relation $\Delta H_0/b \approx 2.5$ K provides evidence that inhomogeneous broadening does not dominate ΔH_0 in the regime where AFM order occurs at low temperatures. These considerations point out that investigating the spin dynamics in $YbRh_2Si_2$, as characterized by the ratio $\Delta H_0/b \approx 2.5$ K, is better achieved by the ESR under pressure than by the ESR with Co doping where the spin dynamics is obscured by additional disorder-related effects.

V. CONCLUSION

We have studied the effect of hydrostatic pressure $p < 2.9$ GPa and Co doping $0 \leq x \leq 0.195$ on the ESR in $Yb(Rh_{1-x}Co_x)_2Si_2$. Both, hydrostatic pressure and chemical pressure by Co doping lead to qualitatively the same effect, namely, an increase in the linewidth and a decrease in the g factor under pressure while at the same time the Kondo temperature is decreased. The pressure dependence of the linear temperature slope of the linewidth is equivalent to the linewidth behavior of local Gd^{3+} spins serving as diluted ESR probes in Ce-based heavy-fermion compounds.[19] There, the change in the low-temperature slope under pressure is explained by the change in the Kondo temperature. Therefore, the equivalency reveals two conclusions: (i) the ESR in $YbRh_2Si_2$ looks alike a resonance of local Yb^{3+} spins in a metallic environment and (ii) the Kondo temperature is a relevant parameter to describe the linewidth. The present theoretical frameworks for the ESR in $YbRh_2Si_2$ (Refs. 10 and 11) provide a reasonable basis to understand the ESR under pressure in terms of the Kondo effect and the presence of ferromagnetic correlations. The different effect of Co doping and pressure on the linewidth suggests that disorder induced by Co doping is more effective in destroying the lattice coherence, the latter being essential for observing narrow ESR lines in dense Kondo-lattice systems.[11] The linewidth data for all investigated pressures and Co contents could be characterized by a universal ratio between the residual linewidth and the slope of the linear temperature dependence of the linewidth. By relating both quantities to the scattering processes of charge transport the evolution of the ESR data with pressure allow a further characterization of the influence of the Kondo interaction to the ESR of $YbRh_2Si_2$.

ACKNOWLEDGMENTS

This work was supported by the DFG within TRR 80 (Augsburg, Munich), by the Volkswagen Foundation (Grant No. I/82203 and I/84689), and the DFG Research Unit 960 "Quantum Phase Transitions." We acknowledge fruitful discussions with M. Brando.

[1] P. Jarillo-Herrero, J. Kong, H. S. J. van der Zant, C. Dekker, L. P. Kouwenhoven, and S. De Franceschi, Nature (London) **434**, 484 (2005).
[2] J. Sichelschmidt, V. A. Ivanshin, J. Ferstl, C. Geibel, and F. Steglich, Phys. Rev. Lett. **91**, 156401 (2003).
[3] C. Krellner, T. Förster, H. Jeevan, C. Geibel, and J. Sichelschmidt, Phys. Rev. Lett. **100**, 066401 (2008).
[4] U. Schaufuß, V. Kataev, A. A. Zvyagin, B. Büchner, J. Sichelschmidt, J. Wykhoff, C. Krellner, C. Geibel, and F. Steglich, Phys. Rev. Lett. **102**, 076405 (2009).
[5] H.-A. Krug von Nidda, A. Schütz, M. Heil, B. Elschner, and A. Loidl, Phys. Rev. B **57**, 14344 (1998).
[6] E. Abrahams and P. Wölfle, Phys. Rev. B **78**, 104423 (2008).
[7] A. A. Zvyagin, V. Kataev, and B. Büchner, Phys. Rev. B **80**, 024412 (2009).
[8] P. Schlottmann, Phys. Rev. B **79**, 045104 (2009).
[9] D. L. Huber, J. Phys.: Condens. Matter **21**, 322203 (2009).
[10] B. I. Kochelaev, S. I. Belov, A. M. Skvortsova, A. S. Kutuzov, J. Sichelschmidt, J. Wykhoff, C. Geibel, and F. Steglich, Eur. Phys. J. B **72**, 485 (2009).
[11] P. Wölfle and E. Abrahams, Phys. Rev. B **80**, 235112 (2009).
[12] P. Gegenwart, Q. Si, and F. Steglich, Nat. Phys. **4**, 186 (2008).
[13] J. Sichelschmidt, J. Ferstl, C. Geibel, and F. Steglich, Physica B **359-361**, 17 (2005).
[14] J. Wykhoff, J. Sichelschmidt, J. Ferstl, C. Krellner, C. Geibel, F. Steglich, I. Fazlishanov, and H.-A. Krug von Nidda, Physica C **460-462**, 686 (2007).
[15] J. G. S. Duque *et al.*, Phys. Rev. B **79**, 035122 (2009).
[16] S. E. Barnes, Adv. Phys. **30**, 801 (1981).
[17] S. Friedemann, T. Westerkamp, M. Brando, N. Oeschler, S. Wirth, P. Gegenwart, C. Krellner, C. Geibel, and F. Steglich, Nat. Phys. **5**, 465 (2009).
[18] M. A. Continentino, B. Elschner, and G. Jakob, Europhys. Lett. **31**, 485 (1995).
[19] M. Schlott and B. Elschner, Z. Phys. B: Condens Matter **78**, 451 (1990).
[20] A. Goltsev and M. Abd-Elmeguid, J. Phys.: Condens. Matter **17**, S813 (2005).
[21] S. Mederle, R. Borth, C. Geibel, F. Grosche, G. Sparn, O. Trovarelli, and F. Steglich, J. Phys.: Condens. Matter **14**, 10731

(2002).
[22] Y. Tokiwa, P. Gegenwart, T. Radu, J. Ferstl, G. Sparn, C. Geibel, and F. Steglich, Phys. Rev. Lett. **94**, 226402 (2005).
[23] O. Trovarelli, C. Geibel, S. Mederle, C. Langhammer, F. M. Grosche, P. Gegenwart, M. Lang, G. Sparn, and F. Steglich, Phys. Rev. Lett. **85**, 626 (2000).
[24] C. Krellner, Ph.D. thesis, Technische Universität Dresden, 2009.
[25] C. Klingner, Diploma thesis, Technische Universität Dresden, 2009.
[26] N. Preusse, Ph.D. thesis, Technische Hochschule Darmstadt, 1987.
[27] J. Wykhoff, J. Sichelschmidt, G. Lapertot, G. Knebel, J. Flouquet, I. I. Fazlishanov, H.-A. Krug von Nidda, C. Krellner, C. Geibel, and F. Steglich, Sci. Technol. Adv. Mater. **8**, 389 (2007).
[28] D. Zakharov, D. G. Zverev, and V. V. Izotov, JETP Lett. **78**, 402 (2003).
[29] J. Plessel, M. M. Abd-Elmeguid, J. P. Sanchez, G. Knebel, C. Geibel, O. Trovarelli, and F. Steglich, Phys. Rev. B **67**, 180403(R) (2003).
[30] P. Gegenwart *et al.*, New J. Phys. **8**, 171 (2006).
[31] C. Klingner, C. Krellner, and C. Geibel, J. Phys.: Conf. Ser. **200**, 012089 (2010).
[32] A. Kutuzov, A. Skvortsova, S. Belov, J. Sichelschmidt, J. Wykhoff, I. Eremin, C. Krellner, C. Geibel, and B. Kochelaev, J. Phys.: Condens. Matter **20**, 455208 (2008).